# TREE SPECIES CLASSIFICATION OF INDIVIDUAL TREES IN SWEDEN BY COMBINING HIGH RESOLUTION LASER DATA WITH HIGH RESOLUTION NEAR-INFRARED DIGITAL IMAGES

Å. Persson [a], J. Holmgren [b], U. Söderman [a], and H. Olsson [b]

[a] Department of Laser Systems, Swedish Defence Research Agency, P.O. Box 1165, SE-58111 Linköping, Sweden - (asa.persson, ulf.soderman)@foi.se

[b] Department of Forest Resource Managements and Geomatics, Swedish University of Agricultural Sciences, SE-90183 Umeå, Sweden - (johan.holmgren, hakan.olsson)@resgeom.slu.se

**KEY WORDS**: Aerial digital images, Airborne laser scanning, Data fusion, Forest inventory, LIDAR, Tree species classification

**ABSTRACT:**

The aim of this research is to make identification of tree species of individual trees more efficient through combining high resolution laser data with high resolution near-infrared images. Identification of the classes Scots pine (*Pinus silvestris* L.), Norway spruce (*Picea abies* L.), and deciduous trees was chosen because these groups are the most important for forest applications in Sweden. Tree species classification is the last step in a method that has the following steps: (1) delineation of individual tree crowns using laser data, (2) estimation of tree height and crown area using laser data, and finally (3) species identification of the delineated tree crowns by adding data from near-infrared digital images. The tests were performed in southern Sweden at the Remningstorp test site (lat. 58°30'N, long. 13°40'E). The laser measurements had a density of seven laser measurements per square meter and the near-infrared images had a pixel size of 10 cm. On ground, tree position and stem diameter were measured and tree species recorded for trees within a Scots pine dominated, a Norway spruce dominated, and a birch dominated forest stand. Near-infrared images were used for classification. The camera position and orientation of each image was used to map laser generated tree segments to the corresponding pixels in the aerial image. The results indicate that near-infrared images add useful information for tree species classification.

## 1. INTRODUCTION

Airborne laser scanning can be used to first detect individual trees and then measure the detected trees (Hyyppä & Inkinen, 1999; Hyyppä et al., 2001; Persson et al., 2002; Schardt et al., 2002). Position and tree height of individual trees can be estimated with sub-meter accuracy. This ability will allow for high precision forest inventories and thereby also more efficient utilization of forest resources. The next step is to identify the species of the detected trees. Properties of laser data within segments of individual trees have been used for separation of Norway spruce (*Picea abies* L.) and Scots pine (*Pinus Sylvestris* L.) with 95 % accuracy (Holmgren & Persson, 2004). Further information can be achieved by fusion with data from other sensors. Fused data sets are the most information-rich data products created from lidar-derived elevation data (Flood, 2002). High density laser data is powerful for tree canopy delineation and for assessing canopy shape, while spectral properties can be extracted from digital images. Near-infrared images are useful for separating between coniferous and deciduous trees (Lillesand & Kiefer, 1994). Because the Swedish forests mostly consist of Norway spruce, Scots pine, and deciduous trees, classification into these groups is important for forest applications. The objective with this study is therefore to investigate how near-infrared images can be used together with laser data in order to classify individual trees into the groups Norway spruce, Scots pine, and deciduous trees.

## 2. MATERIAL

The test site, Remningstorp, is located in the south of Sweden (lat. 58°30', long. 13°40'). The dominant tree species are Norway spruce (*Picea abies* L.), Scots pine (*Pinus sylvestris* L.) and birch (*betula* spp.). The dominant soil type is till with a field layer consisting of blueberry (*Vaccinium myrtillus*) and cowberry (*Vaccinium vitis-idaea*). The ground elevation is moderately varying between 120 and 145 m above sea level.

### 2.1 Laser data

The laser data acquisition was performed the 11th of August 2003. The flight height was 130 m, flight speed 16 $ms^{-1}$, scan angle ±20 degrees, and pulsing frequency 7000 Hz. The swaths were overlapping which resulted in an average measuring density of approximately seven laser measurements per square-meter. The beam divergence of the laser (1064 nm) was 1 mrad and both the first and last return pulses were recorded.

### 2.2 Near infrared images

Digital images were recorded using the Digital Mapping Camera (DMC) the 14th of October 2003. The DMC camera comprises eight synchronously operating CCD-matrix based camera modules. Four panchromatic images from these cameras are used for creating a single high resolution image. Additionally, four parallel cameras can generate multi-spectral images (Heier & Hinz, 2002). The images are 12 bits (4096 digital levels) but stored as 16 bit images. The four panchromatic cameras produced virtual images of 13824×7680 pixels (focal length: 120 mm, resolution: 12 µm). Three multi-spectral cameras were used that were sensitive in the spectral bands B1 (500-650 nm), B2 (590-675 nm), and B3 (675-850 nm). The multi-spectral cameras produced lower resolution images of 3072×2048 pixels (focal length: 25 mm, resolution: 12 µm). The images that were used for these tests are compositions of the high resolution panchromatic image (0.1 m pixel size on ground) and the multi-spectral image (CIR) (0.6 m

pixel size on ground). The following steps were used to set color data to the high resolution image: (1) the multi-spectral image was resampled to the resolution of the panchromatic image (PAN), (2) RGB to IHS color transformation was applied to the CIR image, (3) the intensity channel was replaced by the PAN image, and (4) the inverse color transformation (IHS to RGB) was applied. Block triangulation was performed to calculate the exterior orientation parameters. Ground control points were used that had been linked to the measured tree positions using a total station. Only terrestrial measured plane coordinates were available and therefore laser measurements were used for deriving z-coordinates.

### 2.3 Field data

Three 80×80 $m^2$ plots, each dominated by Norway spruce, Scots pine or deciduous trees, were used for the tests reported in this paper. On each plot, the position of the centre of the tree stems in a local coordinate system was measured (1.3 m above ground) using an electronic total station. Positions of trees were measured relatively reference points and the positions of reference points were measured using RTK-GPS. The stem diameter (1.3 m above ground) was measured and tree species was recorded for all trees. For randomly selected sample trees, the tree height and crown base height were measured using an angle hypsometer.

## 3. METHODS

The method to classify trees has the following steps: (1) individual tree crowns are delineated using laser data, (2) the height and crown diameter are measured for each tree, and finally (3), the tree species are classified. In this work, the classification is based on near-infrared images.

### 3.1 Delineation of individual tree crowns

An earlier developed method for detection of individual trees and measuring tree height and crown diameter has the following steps: (1) a digital surface model (*DSM*) is created, (2) a digital terrain model (*DTM*) is created, (3) a digital canopy model (*DCM*) is created, (4) the *DCM* is filtered with different Gaussian filters resulting in different images, (5) the different images are segmented separately and the segment chosen for a specific area is selected though fitting a parabolic surface to the laser data (Persson et al., 2002).

### 3.2 Estimation of tree attributes

The height and crown diameter are derived for the identified trees. In addition, using the tree height and crown diameter, it is possible to derive the stem diameter and timber volume.

### 3.3 Classification of tree species using near-infrared images

Near-infrared images from the DMC camera were used for tree species classification. One image covered both the Norway spruce stand and the Scots pine stand and the other image covered the deciduous forest stand. To avoid re-sampling of the images, the original images were used by back-projecting the laser data to the image according to Equation 1. Using the exterior orientation parameters (camera position ($X_0$, $Y_0$, $Z_0$) and orientation (*omega*, *phi*, and *kappa*)), each tree segment was mapped to the corresponding pixels in the aerial image. Each pixel within an extracted crown segment ($X_p$, $Y_p$, $Z_p$) in the laser data was back-projected to the image ($x_p$, $y_p$)

$$x_p - x_0 = -f\left[\frac{m_{11}(X_p - X_0) + m_{12}(Y_p - Y_0) + m_{13}(Z_p - Z_0)}{m_{31}(X_p - X_0) + m_{32}(Y_p - Y_0) + m_{33}(Z_p - Z_0)}\right] \quad (1)$$

$$y_p - y_0 = -f\left[\frac{m_{21}(X_p - X_0) + m_{22}(Y_p - Y_0) + m_{23}(Z_p - Z_0)}{m_{31}(X_p - X_0) + m_{32}(Y_p - Y_0) + m_{33}(Z_p - Z_0)}\right]$$

where **M** is a 3x3 rotation matrix containing trigonometric expressions of the orientation angles, and $f$ and ($x_0$, $y_0$) the focal length and principal point of the camera respectively.

The spectral information within the crown segments of the images were used to separate between tree species. The illumination can vary between and within crown segments. Depending on the sun position and the structure and size of trees, trees have different shadings. To reduce the effect of shadows, the image can be filtered using band ratio methods (e.g., Quackenbush et al., 2000). An example of a transformation is

$$b_{1out} = \frac{b_1}{\sqrt{b_1^2 + b_2^2 + b_3^2}} \quad (2)$$

$$b_{2out} = \frac{b_2}{\sqrt{b_1^2 + b_2^2 + b_3^2}}$$

$$b_{3out} = \frac{b_3}{\sqrt{b_1^2 + b_2^2 + b_3^2}}$$

where $b_1$, $b_2$, and $b_3$ correspond to the three bands of the original image and $b_{1out}$, $b_{2out}$, and $b_{3out}$ are the bands of the filtered image. Similar, using the ratio of bands, each pixel can be described by two angles in the three dimensional (3D) space, azimuth ($a$) and elevation angle ($e$), thus reducing Equation 2 to two dimensions (2D) according to Equation 3.

$$e = \sin^{-1}\left(\frac{b_3}{\sqrt{b_1^2 + b_2^2 + b_3^2}}\right) = \sin^{-1}(b_{3out}) \quad (3)$$

$$a = \tan^{-1}\left(\frac{b_2}{b_1}\right) = \tan^{-1}\left(\frac{b_{2out}}{b_{1out}}\right)$$

The following steps were used for deriving variables for the classification: (1) the magnitude of each pixel was calculated, (2) the 10% brightest pixels of each crown were extracted, (3) each extracted pixel within a crown segment was described by the azimuth and elevation angle, (4) and finally, the mean value of the azimuth and elevation angle within each segment was derived. The selection of the 10% brightest pixels was motivated by segmentation errors along borders of crown segments. For example, some segments were too large, because they included ground pixels within segments.

### 3.4 Liking remote sensing data and field measurements

The laser detected trees were linked to the field measured trees using the field measured and laser measured tree position. For each extracted crown segment in the laser data, the closest field

measured tree (x, y-distance) that fulfilled the height restriction and was within the segment was linked to a specific laser detected tree. The height restriction was applied in order to reduce linking errors: trees were not linked if the height of the field tree was more than 1.5 times smaller than the laser estimated tree height. The height of non-sample field trees was estimated using a simple function relating tree height to stem diameter. After linking of laser detected and field measured trees, an evaluation of the results on an individual tree basis was performed.

## 4. RESULTS AND DISCUSSION

The aerial image of a Norway spruce stand in Figure 1 (upper left) shows that the illumination is different within and between the extracted crown segments. Applying the filtering step (Equation 2) to the near-infrared image, resulted in more evenly distributed pixel values for the crown segments (Figure 1, upper right and bottom).

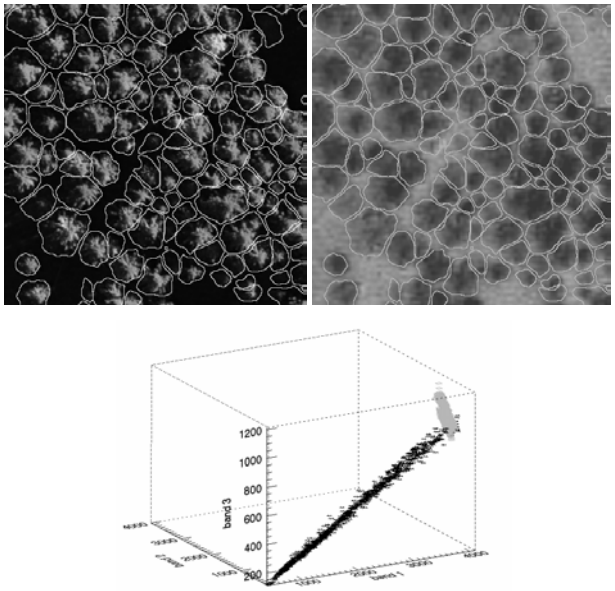


Figure 1. Upper left: Near-infrared image. Upper right: Filtered image. Bottom: Pixel values within one segment, near-infrared image (*) and filtered image (□).

The linking of remote sensing data and field measurements made it possible to plot the variables derived from the aerial image for groups of different tree species (Figure 2). Deciduous trees were separated from coniferous trees in 2D space. However, spectral properties of the deciduous trees depend on the time of the year.

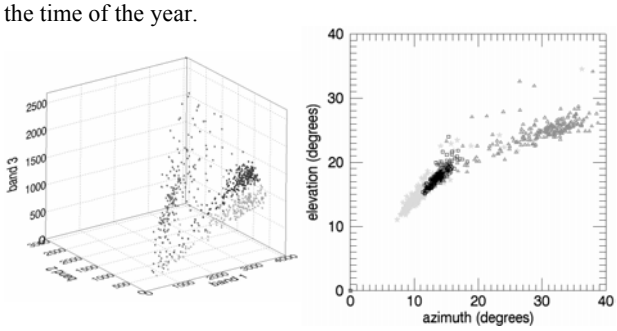


Figure 2. Left: Spectral mean values, Norway spruce (light gray), Scots pine (black), deciduous trees (gray). Right: Azimuth (*a*) and elevation (*e*) angles, Norway spruce (*), Scots pine (□), deciduous trees (Δ).

When applying a quadratic discrimination function to the detected trees with the azimuth (*a*) and elevation angle (*e*) as independent variables, the overall classification accuracy was 90% (Table 1).

| Field registered tree species group | | | |
|---|---|---|---|
| | Scots pine | Norway spruce | Deciduous |
| Scots pine | 222 | 30 | 8 |
| Norway spruce | 13 | 171 | 6 |
| Deciduous | 2 | 10 | 212 |
| Total number | 237 | 211 | 226 |
| Number correct | 222 | 171 | 212 |
| Proportion | 0.94 | 0.81 | 0.94 |
| Overall accuracy = (222 + 171 + 212) / 674 = 90% | | | |

Table 1. Error matrix from the tree species classification.

## 5. CONCLUSIONS

The results indicate that colour near-infrared images are useful for tree species classification. In order to make any conclusions about what accuracy can be expected in an operational case, the validation needs to be extended to also include separate stands that are not used in the training dataset in order to make sure that the difference between tree species is not due to differences between forest stands. However, the results in this paper show that the variables used for the classification (angle *a* and *e*) are not very sensitive to different illumination conditions. Future work will concentrate on combining variables derived from laser data and infrared images for the classification.

## REFERENCES

Flood, M. 2002. Product definitions and guidelines for use in specifying lidar deliverables. *Photogrammetric Engineering and Remote Sensing*, 68, pp. 1230-1234.

Heier, H. & Hinz, A. 2002. Results from the Digital Modular Camera DMC. In proceedings ASPRS, Washington D.C., USA.

Holmgren, J. & Persson, Å. 2004. Identifying species of individual trees using airborne laser scanner. *Remote Sensing of Environment*, 90(4), pp. 415-550.

Hyyppä, J. & Inkinen, M. 1999. Detection and estimating attributes for single trees using laser scanner. *The Photogrammetric Journal of Finland*, 16**,** pp. 27-42.

Hyyppä, J., Kelle, O., Lehikoinen, M. & Inkinen, M. 2001. A segmentation-based method to retrieve stem volume estimates from 3-D tree height models produced by laser scanners. *IEEE Transactions on Geoscience and Remote Sensing,* pp. 39**,** 969-975.

Lillesand, T. M. & Kiefer, R. W. 1994. *Remote sensing and image interpretation.* 3rd. edition. John Wiley & Sons, Inc.**,** New York.

Persson, Å., Holmgren, J. & Söderman, U. 2002. Detecting and measuring individual trees using an airborne laser scanner. *Photogrammetric Engineering and Remote Sensing,* 68**,** pp. 925-932.

Quackenbush, L.J., Hopkins, P.F. & Kinn, G.J. 2000. Developing Forestry Products from High Resolution Digital Aerial Imagery. *Photogrammetric Engineering and Remote Sensing,* 66**,** pp.1337-1346.

Schardt, M., Ziegler, M., Wimmer, A., Wack, R. & Hyyppä, J. 2002. Assessment of forest parameters by means of laser scanning. In: (eds.). *Photogrammetric computer vision, ISPRS Commission III Symposium.* Graz, Austria. September 9-13. pp. 302-309.

**ACKNOWLEDGEMENTS**

We thank TopEye for delivering the laser data and the Swedish National Land Survey for delivering the DMC images. Both laser data and field data were financed by the Hildur and Sven Wingquist Foundation.